ACS APPLIED MATERIALS & INTERFACES

Forum Article

www.acsami.org

Detection of microRNA in Tumor Cells using Exonuclease III and Graphene Oxide-Regulated Signal Amplification

Rong-Cing Huang,[†] Wei-Jane Chiu,[†] Yu-Jia Li,[†] and Chih-Ching Huang*[,†,‡,§]

[†]Institute of Bioscience and Biotechnology and [‡]Center of Excellence for the Oceans, National Taiwan Ocean University, Keelung 20224, Taiwan

[§]School of Pharmacy, College of Pharmacy, Kaohsiung Medical University, Kaohsiung 80708, Taiwan

Supporting Information

ABSTRACT: In this study, we developed a label-free, ultrasensitive graphene oxide (GO)-based probe for the detection of oligonucleotides by laser desorption/ionization mass spectrometry (LDI-MS). On the basis of simple $\pi-\pi$ stacking and electrostatic interactions between rhodamine 6G (R6G) and GO, we prepared the nanocomposite R6G-modified GO (R6G-GO). Signal intensities of R6G increased in mass spectra in the presence of single-stranded oligonucleotides under pulsed laser irradiation (355 nm) of R6G-GO. In addition, the signal intensity of R6G was stronger in the presence of short oligonucleotides. Because small oligonucleotides improve the LDI efficiency of R6G on GO, we designed an enzyme-amplified signal transduction probe system for the detection of microRNA (miRNA). After specific digestion of the probe DNA (pDNA) strand from pDNA/miRNA-hybridized complexes by exonuclease III (*Exo* III), the resulting small oligonucleotide fragments increased the R6G signal during LDI-MS of R6G-GO. In addition, the signal intensity of the R6G ions increased with increasing concentrations of the target miRNA. Coupling this enzyme reaction and R6G-GO with LDI-MS enabled the detection of miRNA at concentrations of the femtomolar (fM) level. We also demonstrated the analysis of miRNA in tumor cells and utilized this R6G-GO probe in the detection of a single-nucleotide polymorphism (SNP) in the Arg249Ser unit of the TP53 gene. This simple, rapid, and sensitive detection system based on the coupling of functional GO with LDI-MS appears to have great potential as a tool for the bioanalyses of oligonucleotides and proteins.

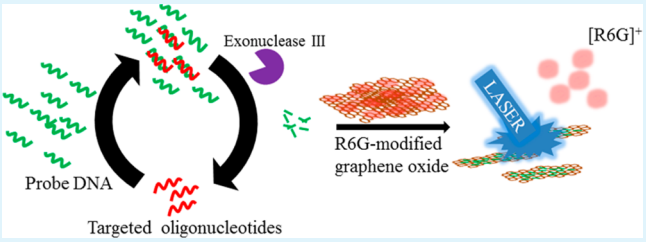

KEYWORDS: *graphene oxide, oligonucleotides, mass spectrometry, microRNA, tumor cells, single-nucleotide polymorphism*

INTRODUCTION

Graphene oxide (GO) is the oxidized counterpart of graphene and consists of a two-dimensional sheet of a mixture of sp^2- and sp^3-hybridized carbon atoms; it has high planar surface and better solubility than graphene.[1,2] Besides being used in optoelectronics, supercapacitors, memory devices, composite materials, and photocatalytic materials, it has recently been considered as a new material for bio-applications such as drug delivery.[3−5] GO possesses a double-sided aromatic scaffold with a high specific surface area of 2630 m^2/g and can afford ultrahigh loading capacity for biomolecules and drugs.[6−8] Moreover, GO has recently been employed as a substrate for the analysis of small molecules, nucleic acids, and proteins in surface-assisted laser desorption/ionization mass spectrometry (SALDI-MS) due to its strong hydrophilicity, efficient energy transfer, and ultrahigh specific surface area.[9−11] It also exhibits a high binding affinity for single-stranded DNA (ssDNA) through $\pi-\pi$ interactions.[12−14] Various dye-labeled ssDNA or aptamers coupled with GO have been developed for the detection of small molecules,[15,16] heavy metal ions,[17,18] proteins, enzymes,[19,20] and oligonucleotides,[21] taking advantage of its high fluorescence quenching efficiency.

Among the several types of polymorphisms that exist in the human genome, single-nucleotide polymorphisms (SNPs) are the most frequent (68%).[22−25] SNP identification is extremely helpful in the diagnosis of genetic diseases, prediction of disease resistance or predisposition, administration of drug dosages, and the design of strategies for personalized medicine.[26] MicroRNAs (miRNAs) are a new class of non-protein-coding, endogenous small RNAs (approximately 19−25 nucleotides in length) that are capable of controlling gene expression by directly interacting with target messenger RNAs (mRNAs).[27] Some miRNAs are known to perform a vital role in various malignancies, either functioning as oncogenes or tumor suppressors.[28] In particular, abnormal expression of miRNAs is commonly observed in cancer initiation, oncogenesis, and tumor response to treatments.[29−32] Therefore, the detection of miRNAs in tumor cells will greatly facilitate the elucidation of

Special Issue: Materials for Theranostics

Received: January 24, 2014
Accepted: April 2, 2014
Published: April 14, 2014

their mechanism and provide effective tools for cellular process control and disease prevention.

In this study, we unveil a new enzyme-amplified signal transduction probe system for the analysis of SNPs and miRNA-34a. First, the designed probe DNA (pDNA) was hybridized with the targeted DNA (tDNA) or miRNA-34a to form pDNA/tDNA or pDNA/miRNA-34a complexes. Next, the pDNA strand was digested by Exonuclease III (*Exo* III) to produce short oligonucleotide fragments and the released tDNA or miRNA-34a were then re-hybridized with the pDNA and reacted with *Exo* III for further amplification (Scheme 1).[33−35] These short oligonucleotides (1−4 mer) can increase laser desorption/ionization (LDI) efficiency of rhodamine 6G (R6G) on GO. Therefore, signal intensity of R6G in laser desorption/ionization mass spectrometry (LDI-MS) of R6G-modified GO (R6G-GO) was increased using higher concentrations of targeted oligonucleotides. Coupling this enzyme reaction and R6G-GO with LDI-MS allowed the detection of miRNA at concentrations of the femtomolar (fM) level. We also demonstrated the analysis of miRNA in tumor cells. Lastly, the R6G-GO/LDI-MS system was used for the detection of SNP in the Arg249Ser unit of the TP53 gene.

Scheme 1. Schematic Representation of Exonuclease III-mediated Signal Amplification Coupled with Laser Desorption/Ionization mass Spectrometry for the Detection of Oligonucleotides

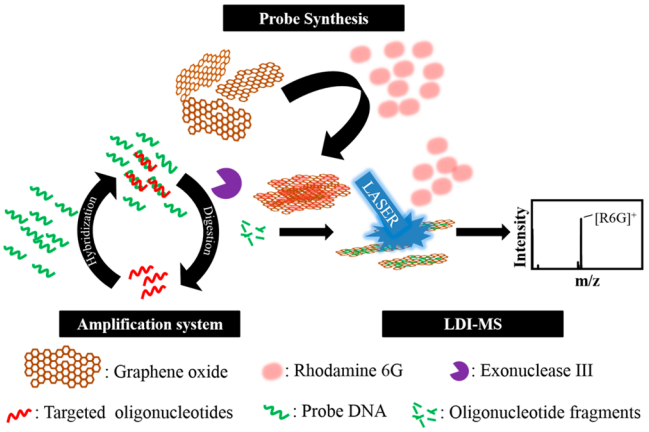

MATERIALS AND METHODS

Chemicals. All DNA and miRNA-34a (sequences listed in Table S1 in the Supporting Information) were purchased from Integrated DNA Technologies (Coralville, IA). Graphite powder (size 7−11 μm), rhodamine 6G, sulfuric acid (H_2SO_4), phosphoric acid (H_3PO_4), hydrogen peroxide (H_2O_2), hydroxydaunorubicin, and *Exo* III (100 unit/μL; 1 unit enzyme digest 1 nmol DNA per 30 min) were purchased from Sigma-Aldrich (Milwaukee, WI). Citric acid, ammonia, calcium chloride ($CaCl_2$), magnesium chloride ($MgCl_2$), potassium permanganate ($KMnO_4$), tris(hydroxymethyl) aminomethane (Tris), and hydrochloric acid (HCl) were purchased from Mallinckrodt Baker (Phillipsburg, NJ). The buffer (ammonium citrate) comprised ammonia and citric acid (1:2). Milli-Q ultrapure water (Millipore, Billerica, MA) was used in all experiments.

Preparation and Characterization of GO. GO was prepared using a modification of the Hummers method.[36,37] Briefly, a 9:1 mixture of concentrated H_2SO_4:H_3PO_4 (360:40 mL) was added to a mixture of 3.0 g of graphite powder and 18.0 g of $KMnO_4$. The reaction was then heated to 50 °C and stirred for 12 h. The reaction was cooled to room temperature in ice and poured onto 100 mL of DI water with 3 mL of 30% H_2O_2. The reaction liquid was then centrifuged at a relative centrifugal force (RCF) of 35,000 g for 1 h, and the supernatant was decanted. The remaining pellet was then repeatedly washed with 200 mL of DI water until a pH level of 6 was reached. After sonication for 1 h, the reaction liquid was centrifuged at a RCF of 25 000 g for 0.5 h to collect the GO solution, and the remaining pellet was discarded. The GO concentration of the supernatant as determined using the freeze dry method was 2.5 g L^{-1} and was denoted as 100×. The dynamic light scattering (DLS) and zeta potential experiments were conducted using a zetasizer 3000HS analyzer (Malvern Instruments, Malvern, UK). Transmission electron microscopy (TEM) was performed using a HT-7700 system (HITACHI, JP) operated at 75 kV.

Preparation and Characterization of R6G-GO. The R6G-GO composite (100×) was prepared by mixing the GO (100X) and R6G (15 μM) in DI water and incubating for 1 h at room temperature. To study the fluorescence quenching efficiency of GO to R6G, 500 μL aliquots of the ammonium citrate solution (50 mM, pH 8) containing GO (250 mg·L^{-1}) and R6G (1.5 μM) were prepared and incubated for 1 h. The mixtures (200 μL) were then transferred separately into 96-well plates, where their fluorescence spectra were recorded using a Synergy 4 Multi-Mode microplate spectrophometer (Biotek Instruments, Winooski, VT) at an excitation wavelength of 510 nm. For determining the maximum amount of the absorption (B_{max}) and Langmuir equilibrium constant (K_{abs}) of GO for R6G, 500 μL aliquots of the ammonium citrate solution (50 mM, pH 8) containing GO (25 mg L^{-1}) and R6G (0−2.0 μM) were prepared and incubated for 1 h. The mixtures (200 μL) were then transferred separately into 96-well plates, where their fluorescence spectra were recorded using a Synergy 4 Multi-Mode microplate spectrophometer.

Analysis of Oligonucleotides. *Exo* III digestion of the probe DNA was performed in a digestion buffer [25 mM Tris-HCl buffer (pH 7.6) containing 1 mM $MgCl_2$ and $CaCl_2$] at 37 °C. First, the probe DNA (0−10 nM) and *Exo* III (5 U) were mixed in the digestion buffer (100 μL) and then different concentrations of the target DNA or RNA in digestion buffer were added to the solution and incubated at 37 °C for 1 h. The solutions were then separately incubated with R6G-GO in 5 mM ammonium citrate solution (pH 8) at room temperature for 30 min. A portion of the samples (approximately 2.0 μL) was cast onto a stainless steel 384-well MALDI target and air-dried at room temperature prior to LDI-time-of-flight (TOF) MS measurements. MS experiments were performed in the reflectron positive-ion mode using an Autoflex III MALDI TOF/TOF mass spectrometer (Bruker Daltonics, Bremen, Germany). The samples were irradiated using a SmartBeam laser (355 nm Nd: YAG) at 100 Hz. Ions produced by laser desorption and ionization were energetically stabilized during a delayed extraction period of 30 ns and accelerated through the TOF chamber in the reflection mode before entering the mass analyzer. The available accelerating voltages ranged from +20 to −20 kV. The instruments were calibrated with Au clusters using their theoretical mass values ($[Au_n]^+$; n = 1−3) before the analysis. A total of 500 pulsed laser shots were applied to accumulate signals from five MALDI target positions at a power density of 3.31×10^4 W cm^{-2}.

Cell Culture and Preparation of Cellular Extracts. Cancer cell lines (MDA-MB-231, MCF-7, HCT-116, A549) and immortalized normal mammary epithelial cell line (MCF-10a) were purchased from the American Type Culture Collection (Manassas, VA). Briefly, the cells were maintained in Dulbecco's modified Eagle's medium supplemented with 10% fetal bovine serum (GIBCO, Campinas, Brazil). MCF-10a cells were cultured in alpha-MEM (GIBCO) supplemented with pre-qualified human recombinant epidermal growth factor 1-53 (EGF 1-53; Invitrogen, Carlsbad, CA) and bovine pituitary extract (Invitrogen). HCT-116 cells were cultured as described by Waldman et al.[38] and treated with 0.2 μg mL^{-1} hydroxydaunorubicin for 1 h to induce miRNA-34a overexpression. All cells were cultured in a humidified incubator at 37 °C containing 5% CO_2. The preparation of cellular extracts was conducted according to a TRIzol® reagent method.[39] Briefly, approximately 1×10^7 cells were washed once with phosphate buffered saline (PBS; pH 7.4,

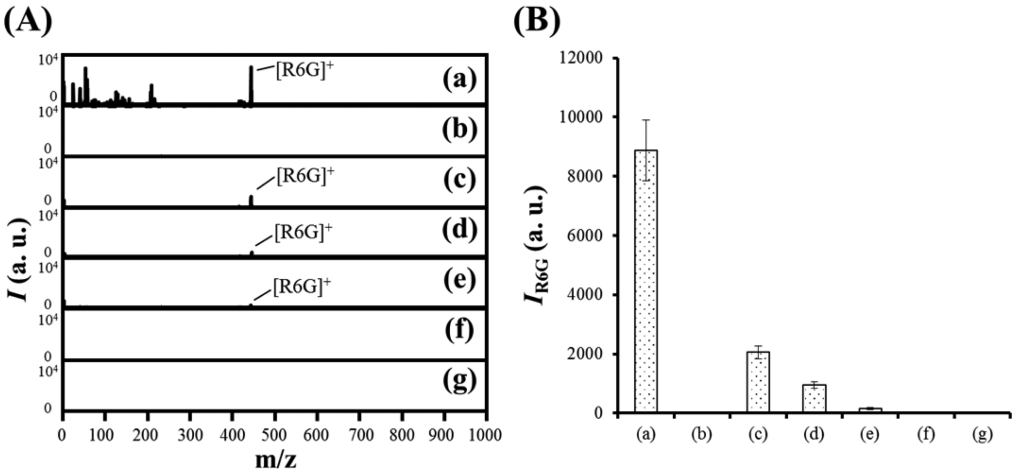

Figure 1. (A) LDI-MS spectra and (B) R6G peak intensity (I_{R6G}) of ammonium citrate solution (50 mM, pH 8) containing (a) R6G (1.5 μM), (b–g) R6G (1.5 μM) and GO (10X) in the absence (b) and presence (c–g) of (c) dNTP, (d) ssDNA4-mer, (e) ssDNA15-mer, (f) ssDNA25-mer, and (g) ssDNA50-mer. Signal at m/z 443.23 was assigned to the $[R6G]^+$ ion. A total of 500 pulsed laser shots were applied to accumulate the signals from five LDI target positions at a laser power density of 3.31 × 10^4 W cm^{-2}. Peak intensities (I) are plotted in arbitrary units (a.u.).

containing 137 mM NaCl, 2.7 mM KCl, 10 mM Na_2HPO_4, and 2.0 mM KH_2PO_4) and total RNA was then extracted using TRIzol reagent (Invitrogen), following the manufacturer's instructions.[39] All RNA samples were split into small aliquots and stored at −80 °C until analysis.

RESULTS AND DISCUSSION

LDI-MS of R6G-GO. Prepared R6G-GO substrates through simple π–π stacking and electrostatic interactions between R6G and GO. First, GO was synthesized from graphite (7–11 μm) using a modified Hummers method.[36,37] Atomic force microscopy (AFM) and transmission electron microscopy (TEM) studies showed that the average size of a single-layer GO was approximately 235 nm, with a thickness of approximately 1.2 nm (see Figure S1A, B in the Supporting Information).[40] Furthermore, Raman spectroscopy showed highly ordered GO-specific bands in its spectra, the in-phase vibration of the graphene lattice (G band, sp^2) at 1575 cm^{-1}, and a (weak) disorder band caused by the graphene edges (D band, sp^3) at approximately 1355 cm^{-1} (see Figure S1C in the Supporting Information).[41] We also noted that GO [10×; the concentration of the prepared GO was denoted as 100× (2.5 g L^{-1})] greatly quenched the fluorescence intensity of R6G (1.5 μM) in ammonium citrate solution (50 mM, pH 8) by transferring energy between R6G and the GO (see Figure S2 in the Supporting Information). We estimated the quenching constant of GO for R6G (13.80 mg^{-1} L) using the following Stern–Volmer equation: $I_{F0}I_F^{-1} = 1 + K_{sv}[Q]$, in which I_{F0} and I_F are the fluorescence of R6G intensities at 554 nm in the absence and presence of GO, respectively; K_{sv} is the Stern–Volmer quenching constant; and [Q] is the concentration of GO (see Figure S3 in the Supporting Information). The properties of high binding affinity and strong electron transfer were mainly responsible for this ultrahigh quenching constant.[42,43] Using the Langmuir absorption isotherm model, the maximum amount of absorption (B_{max}) and Langmuir equilibrium constant (K_{abs}) of GO (1X) for R6G were 0.49 μg g^{-1} and 0.95 μM^{-1} (see Figure S4 in the Supporting Information), respectively.

As shown in Figure 1, the ionization and desorption efficiency of R6G was highly suppressed after GO absorption using pulse laser irradiation (355 nm Nd:YAG, 100 Hz, pulse width 6 ns, laser power density of 3.31 × 10^4 W cm^{-2}). This phenomenon may be attributable to the strong interaction between R6G molecules and GO. R6G (1.5 μM) induced the aggregation of GO (10×) in ammonium citrate solution (TEM images shown in Figure 2B). The zeta potentials and hydrodynamic diameters of GO and R6G-GO were measured to be −49.70 ± 2.02 mV/278 ± 14 nm and −18.03 ± 6.02

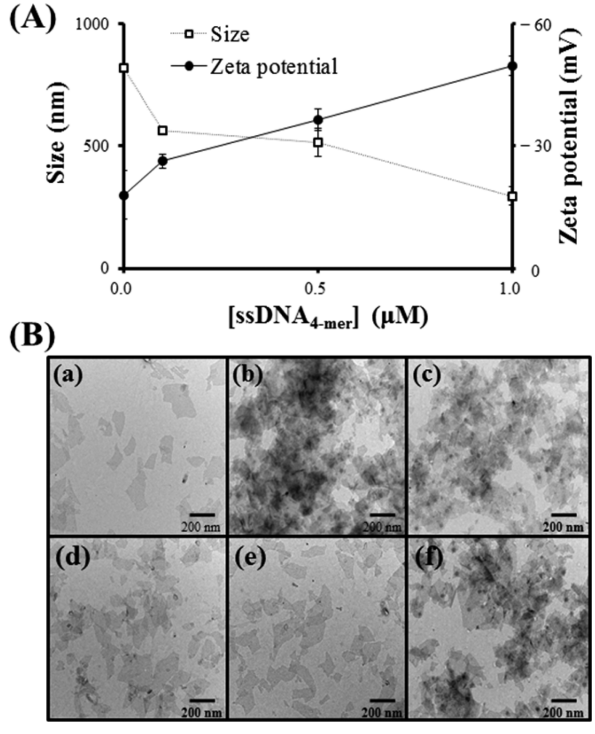

Figure 2. (A) DLS sizes and zeta-potentials of R6G-GO in the presence $ssDNA_{4\text{-mer}}$ (0–1.0 μM) and (B) TEM images of (a) GO, (b–f) R6G-GO in the absence (b) and presence (c–f) of (c) 0.1 μM $ssDNA_{4\text{-mer}}$, (d) 0.5 μM $ssDNA_{4\text{-mer}}$, and (e) 1.0 μM $ssDNA_{4\text{-mer}}$, and (f) 1.0 μM $ssDNA_{50\text{-mer}}$. The GO (10X) or R6G-GO (prepared from 1.5 μM R6G and 10X GO) in the absence and presence of ssDNA were prepared in ammonium citrate solution (50 mM, pH 8). Other conditions were the same as those described in Figure 1

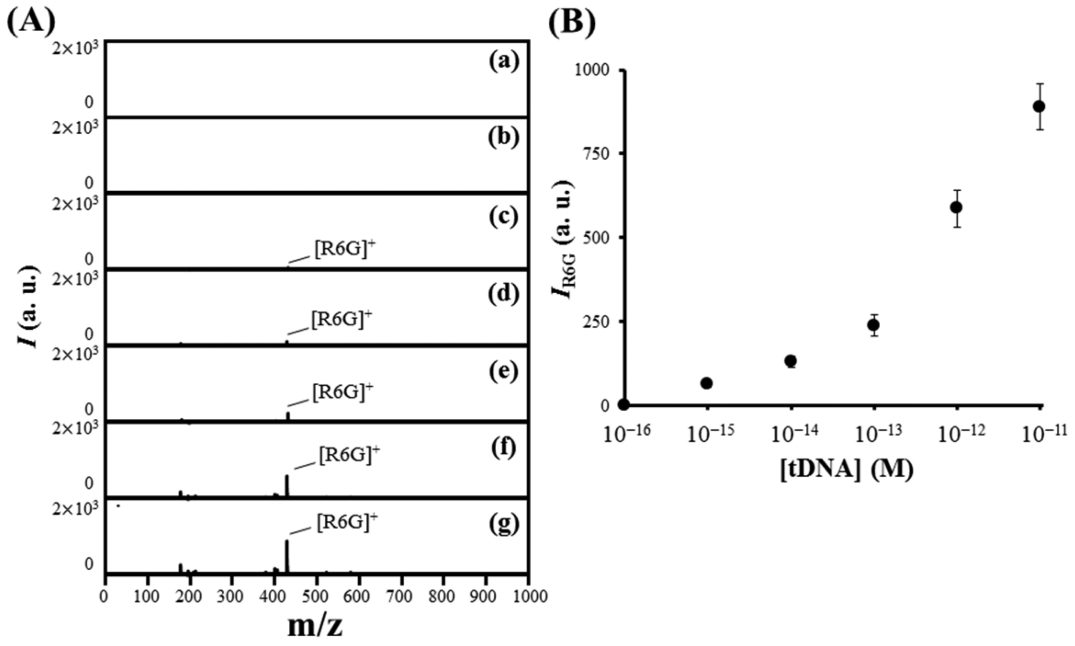

Figure 3. (A) LDI-MS spectra recorded using the *Exo* III-pDNA/R6G-GO as a probe for the detection of (a) 0, (b) 0.1 fM, (c) 1.0 fM, (d) 10.0 fM, (e) 100.0 fM, (f) 1.0 pM, and (g) 10 pM tDNA. (B) The mass signal intensity of $[R6G]^+$ (I_{R6G}) with respect to the tDNA concentration (0−10 pM). Error bars in B represent standard deviations from four repeated experiments. Other conditions were the same as those described in Figure 1.

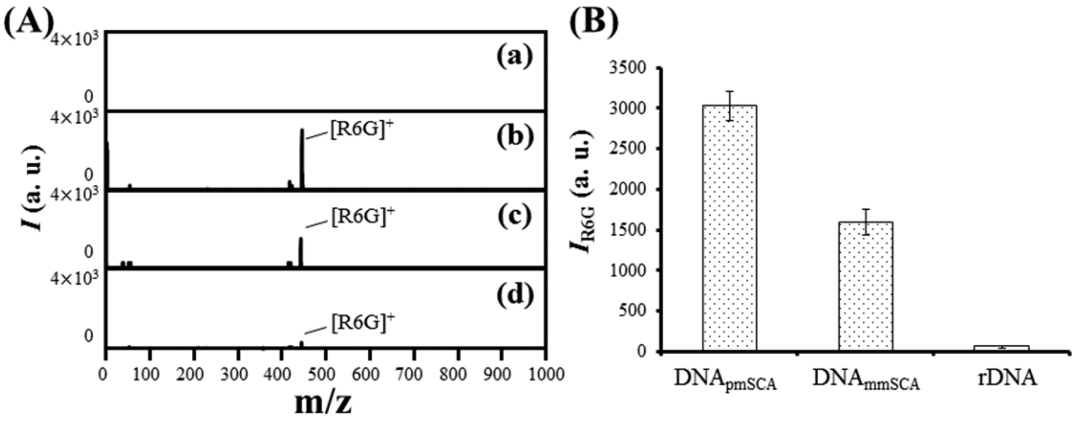

Figure 4. (A) LDI-MS spectra of *Exo* III-pDNA$_{SCA}$/R6G-GO probe in the (a) absence and (b−d) presence of (b) DNA$_{pmSCA}$ (10 pM), (c) DNA$_{mmSCA}$ (10 pM), and (d) rDNA (10 pM). (B) Plots of $[R6G]^+$ peak intensity (I_{R6G}) in the presence of DNA$_{pmSCA}$, DNA$_{mmSCA}$, or rDNA. Error bars in (B) represent standard deviations from four repeated experiments. Other conditions were the same as those described in Figure 3.

mV/822 ± 52 nm, respectively. GO has good solubility in the aqueous medium because of the presence of hydroxyl and carboxylate groups on its surfaces. However, the zeta potential of GO decreased when R6G molecules were absorbed on its surfaces, resulting in GO aggregation. The aggregated GO may have reduced the accessibility of laser light to the absorbed R6G molecules, and it may have lowered desorption/ionization efficiency. The deoxyribonucleotide triphosphates (dNTPs) or short chain ssDNA (4-mer ssDNA; denoted as ssDNA$_{4\text{-mer}}$; sequence listed in Table S1 in the Supporting Information) interacted with R6G-GO, further enhancing the peak intensity of R6G in the LDI-MS spectra (Figure 1). We conducted the dynamic light scattering (DLS) and TEM measurements to characterize R6G-GO in the presence of ssDNA$_{4\text{-mer}}$ at various concentrations, ranging from 0 to 1.0 μM (Figure 2 and Figure S5 in the Supporting Information). The DLS size of R6G-GO decreased, whereas the zeta potential increased with higher concentrations of ssDNA$_{4\text{-mer}}$ (Figures 2A and Figure S5 in the Supporting Information). TEM images further confirmed the improvement in dispersion of R6G-GO with higher concentrations of ssDNA$_{4\text{-mer}}$ (Figure 2B b−e). In contrast, the degree of aggregation of R6G-GO was not affected by ssDNA$_{50\text{-mer}}$ (Figure 2Bf). The short-chained ssDNA has easy access to the R6G-unoccupied surface of GO. Therefore, we inferred that the difference in the R6G signal strength in the LDI-MS was influenced by the degree of aggregation of R6G-GO. The shorter ssDNA played a significant role in separating the R6G-GO sheets from the aggregates and facilitated increased dispersion. In addition, we suspect that when longer ssDNA strands adsorb onto the surfaces of GO, the transfer of laser energy from GO to DNA is easier, resulting in a decrease in R6G desorption efficiency. It also cannot be ruled out that the surface of GO in the presence of longer ssDNA may inhibit the ionization ability of R6G.

LDI-MS Coupled with Cyclic Enzyme Amplification. To increase the sensitivity of the R6G-GO probe for the detection

of oligonucleotides, *Exo* III-mediated signal amplification was performed (Scheme 1). Target oligonucleotide (ssDNA or miRNA)-hybridized pDNA was digested using *Exo* III, the released ssDNA or miRNA could again hybridize with other pDNA molecules for subsequent *Exo* III digestion, thus increasing oligonucleotide fragments concentration and consequently enhancing the R6G signal during LDI-MS of R6G-GO. This signal amplification system enabled the detection of target DNA (tDNA; sequence listed in Table S1 in the Supporting Information) to levels as low as 1.0 fM (Figure 3). Compared with other GO-based sensors for the detection of oligonucleotides, the *Exo* III-pDNA/R6G-GO probe is relatively simple, rapid, and cost-effective. Most detection techniques require covalent conjugation of a dye or electroactive molecules to oligonucleotides or GO.[44−48] We further applied our R6G-GO signal amplification system coupled with LDI-MS to detect SNPs that were associated with the development of sickle-cell anemia (SCA).[49] A single A → T transversion in sequence-encoding codon 6 of the human β-globin gene causes an amino acid change from glutamine to valine, resulting in the mutant globin chain, hemoglobin S (HbS). Production of HbS results in irregularly shaped erythrocytes and reduced hemoglobin solubility at low oxygen tension.[50] The sequence of the new probe DNA ($pDNA_{SCA}$) was complementary to that of the wild type (perfectly matched DNA, DNA_{pmSCA}). Figure 4 shows that the probe exhibited a >2-fold and >45-fold selectivity toward DNA_{pmSCA} over a single-base mismatched DNA (DNA_{mmSCA}) and random sequence DNA (rDNA), respectively. Therefore, SNP detection was readily observable by monitoring the R6G signal at room temperature, circumventing the requirement of temperature control that is often associated with specific nanoparticle-based optical and electrochemical sensors.[51−54] We believe that this approach can serve as a foundation for the development of more practical DNA chips for high-throughput SNP screening in various genetic diseases and cancers.

Analysis of miRNA. We further applied our probe to the analysis of miRNA-34a, which is transcriptionally regulated by the p53 network and is associated with cancer cell growth and proliferation in a variety of cancers. miRNA-34a can regulate various mRNAs involved in the cell cycle, cell proliferation, senescence, migration, and invasion such as cyclin-dependent kinase 4/6 (CDK4/6), E2F transcription factor 3 (E2F3), cyclin E2, hepatocyte growth factor receptor (MET), B-cell lymphoma 2 (Bcl-2), NAD-dependent deacetylase sirtuin-1 (SIRT1), and CD44.[55] In the some cancer cells, miRNA-34a expression is significantly decreased.[56] Overexpression of miRNA-34a could inhibit cancer cell migration and invasion *in vitro* and distal pulmonary metastases *in vivo*; therefore, many studies have investigated miRNA-34a levels in cancer cells. Table S1 in the Supporting Information presents the sequence of the probe DNA ($pDNA_{miRNA\text{-}34a}$) that we used as the new probe, *Exo* III-$pDNA_{miRNA\text{-}34a}$/R6G-GO, for the detection of miRNA-34a. The LDI-MS-coupled cyclic enzyme amplification allowed the detection of miRNA-34a at levels as low as 1.0 fM (see Figure S6 in the Supporting Information).

We further applied this detection system to analyze miRNA-34a in five human cell lines, normal mammary epithelial cells (MCF-10a), breast adenocarcinoma cells (MCF-7 and MDA-MB-231), adenocarcinoma alveolar basal epithelial cells (A549), and colorectal carcinoma cells (HCT-116). miRNA-34a expression in these five different cell lysate samples was determined using the proposed method. The cell lysates samples were prepared by using a commercial RNA isolation reagent (TRIzol), and quantitation was conducted at a wavelength of 260 nm. Figure 5 shows that miRNA-34a

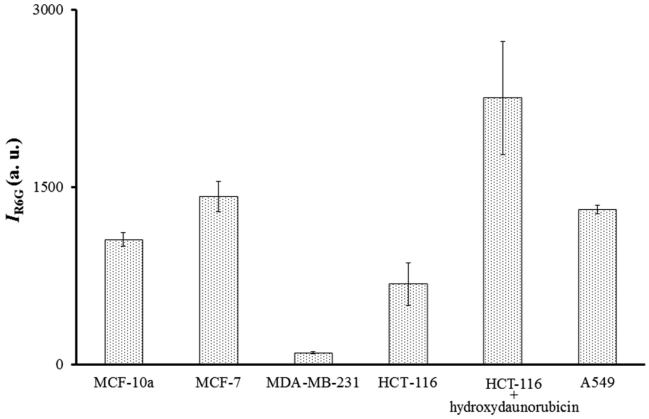

Figure 5. *Exo* III-$pDNA_{miRNA\text{-}34a}$/R6G-GO signal amplification system applied to the detection of miRNA-34a in different cell lysate sample (20 ng μL^{-1}). Error bars represent standard deviations from five repeated experiments.

expression in MDA-MB-231 cells was much lower than that of other cells, in accordance with those obtained from RT-PCR and the northern blotting assay.[57] Moreover, various concentrations of miRNA-34a added to the MCF-7 cell lysates were effectively detected (recovery 90−110%, Figure S7, Supporting Information). The expression of miRNA-34a in MDA-MB231 cells was only 10% of that in MCF-10a cells, in accordance with the fact that miRNA-34a levels were lower in the mesenchymal-type breast cancer cell line (MDA-MB231) when compared with the normal epithelial cell line (MCF-10a).[57,58] Ectopic expression of miRNA-34a in breast cancer cells led to reduced cell proliferation, invasion, and induced apoptosis.[57−59] In addition, the expression of miRNA-34a was up-regulated (Figure 5) after treatment of human colon cancer cells (HCT-116) with the DNA-damaging agent hydroxydaunorubicin (0.2 μg mL^{-1}). It has been previously demonstrated that hydroxydaunorubicin treatment of HCT-116 cells resulted in an increase in p53 and miRNA-34a expression and a decrease in the expression of the SIRT1 protein, which is an NAD-dependent deacetylase that modulates metabolism, inflammation, hypoxic response, circadian rhythm, cell survival, and longevity.[61] miRNA-34a has been identified as a DNA damage-responsive gene in the HCT-116 colon cancer cell line after treatment with DNA-damaging agents, at which cell proliferation is completely arrested without substantial induction of apoptosis.[60] These results indicate that the proposed assay has practical applications in miRNA detection, offering high accuracy and reliability with comprehensive information for the early detection of miRNA-related cancer. Compared with other GO-based sensors for the analysis of miRNA, our *Exo* III-pDNA/R6G-GO probe is relatively simple and low-cost as well as high-throughput, appears to hold great practicality for bioanalyses. Most GO-based detection techniques for miRNA require covalent conjugation of fluorophore molecules to oligonucleotides or GO.[62−68] In addition, these techniques are few applied to determination of miRNA in cancer cells.

CONCLUSIONS

We employed an enzyme-based signal amplification system coupled with LDI-MS for the detection of oligonucleotides. The increase in the R6G signal from the R6G-GO based on the LDI-MS spectra with increasing concentrations of short-length DNA was mainly attributable to the ability of DNA to prevent R6G-GO aggregation. Our proposed probe enables the selective detection of target oligonucleotides down to the fM level. The developed *Exo* III-pDNA$_{miRNA-34a}$/R6G-GO probe has shown efficiency in the analysis of miRNA-34a expression in human cells. We also applied the *Exo* III-pDNA$_{SCA}$/R6G-GO probe for the detection of SNP in the Arg249Ser unit of the TP53 gene, which indicated its potential in studying genetic diseases and cancers. To the best of our knowledge, this study provides the first example of combining enzymatic signal amplification with mass spectrometry for label-free detection of oligonucleotides. This high-throughput LDI-MS-based oligonucleotide detection system shows high potential for oligonucleotide array analysis, and it could be used to detect other biomolecules (e.g., proteins and enzymes)

ASSOCIATED CONTENT

Supporting Information

Supporting Information contains the figures from S1 to S7, which represents the results obtained for AFM, TEM, Raman spectra, fluorescent spectra, Stern−Volmer plots, Langmuir plots, DLS, LDI-MS, and table of oligonucleotides sequences. This material is available free of charge via the Internet at http://pubs.acs.org.

AUTHOR INFORMATION

Corresponding Author

*E-mail: huanging@ntou.edu.tw. Tel.: 011-886-2-2462-2192, ext.: 5517. Fax: 011-886-2-2462-2034;.

Notes

The authors declare no competing financial interest.

ACKNOWLEDGMENTS

This study was supported by the National Science Council of Taiwan under Contract NSC 101-2628-M-019-001-MY3, 102-2113-M-019-001-MY3, and 102-2627-M-019-001-MY3.

REFERENCES

(1) Dreyer, D. R.; Park, S.; Bielawski, C. W.; Ruoff, R. S. The Chemistry of Graphene Oxide. *Chem. Soc. Rev.* **2010**, *39*, 228−240.
(2) Li, D.; Muller, M. B.; Gilje, S.; Kaner, R. B.; Wallace, G. G. Processable Aqueous Dispersions of Graphene Nanosheets. *Nat. Nanotechnol.* **2008**, *3*, 101−105.
(3) Shen, H.; Zhang, L. M.; Liu, M.; Zhang, Z. J. Biomedical Applications of Graphene. *Theranostics* **2012**, *2*, 283−294.
(4) Wang, Y.; Li, Z. H.; Wang, J.; Li, J. H.; Lin, Y. H. Graphene and Graphene Oxide: Biofunctionalization and Applications in Biotechnology. *Trends Biotechnol.* **2011**, *29*, 205−212.
(5) Yang, K.; Feng, L. Z.; Shi, X. Z.; Liu, Z. Nano-Graphene in Biomedicine: Theranostic Applications. *Chem. Soc. Rev.* **2013**, *42*, 530−547.
(6) Patil, A. J.; Vickery, J. L.; Scott, T. B.; Mann, S. Aqueous Stabilization and Self-Assembly of Graphene Sheets into Layered Bio-Nanocomposites Using DNA. *Adv. Mater.* **2009**, *21*, 3159−3163.
(7) Bao, H. Q.; Pan, Y. Z.; Ping, Y.; Sahoo, N. G.; Wu, T. F.; Li, L.; Li, J.; Gan, L. H. Chitosan-Functionalized Graphene Oxide as A Nanocarrier for Drug and Gene Delivery. *Small* **2011**, *7*, 1569−1578.
(8) Zhang, L. M.; Xia, J. G.; Zhao, Q. H.; Liu, L. W.; Zhang, Z. J. Functional Graphene Oxide as A Nanocarrier for Controlled Loading and Targeted Delivery of Mixed Anticancer Drugs. *Small* **2010**, *6*, 537−544.
(9) Dong, X. L.; Cheng, J. S.; Li, J. H.; Wang, Y. S. Graphene as A Novel Matrix for The Analysis of Small Molecules by MALDI-TOF MS. *Anal. Chem.* **2010**, *82*, 6208−6214.
(10) Tang, L. A. L.; Wang, J. Z.; Loh, K. P. Graphene-Based SELDI Probe with Ultrahigh Extraction and Sensitivity for DNA Oligomer. *Chem. Soc.* **2010**, *132*, 10976−10977.
(11) Liu, Q.; Shi, J. B.; Cheng, M. T.; Li, G. L.; Cao, D.; Jiang, G. B. Preparation of Graphene-Encapsulated Magnetic Microspheres for Protein/Peptide Enrichment and MALDI-TOF MS Analysis. *Chem. Commun.* **2012**, *48*, 1874−1876.
(12) Song, B.; Cuniberti, G.; Sanvito, S.; Fang, H. P. Nucleobase Adsorbed at Graphene Devices: Enhance Bio-sensorics. *Appl. Phys. Lett.* **2012**, *100*, 063101.
(13) Manohar, S.; Mantz, A. R.; Bancroft, K. E.; Hui, C. Y.; Jagota, A.; Vezenov, D. V. Peeling Single-Stranded DNA from Graphite Surface to Determine Oligonucleotide Binding Energy by Force Spectroscopy. *Nano Lett.* **2008**, *8*, 4365−4372.
(14) Gowtham, S.; Scheicher, R. H.; Ahuja, R.; Pandey, R.; Karna, S. P. Physisorption of Nucleobases on Graphene: Density-Functional Calculations. *Phys. Rev. B: Condens. Matter Mater. Phys.* **2007**, *76*, 4.
(15) Liu, J. H.; Wang, C. Y.; Jiang, Y.; Hu, Y. P.; Li, J. S.; Yang, S.; Li, Y. H.; Yang, R. H.; Tan, W. H.; Huang, C. Z. Graphene Signal Amplification for Sensitive and Real-Time Fluorescence Anisotropy Detection of Small Molecules. *Anal. Chem.* **2013**, *85*, 1424−1430.
(16) Sheng, L. F.; Ren, J. T.; Miao, Y. Q.; Wang, J. H.; Wang, E. K. PVP-Coated Graphene Oxide for Selective Determination of Ochratoxin A via Quenching Fluorescence of Free Aptamer. *Biosens. Bioelectron.* **2011**, *26*, 3494−3499.
(17) Sudibya, H. G.; He, Q. Y.; Zhang, H.; Chen, P. Electrical Detection of Metal Ions Using Field-Effect Transistors Based on Micropatterned Reduced Graphene Oxide Films. *ACS Nano* **2011**, *5*, 1990−1994.
(18) Wen, Y. Q.; Peng, C.; Li, D.; Zhuo, L.; He, S. J.; Wang, L. H.; Huang, Q.; Xu, Q. H.; Fan, C. H. Metal Ion-Modulated Graphene-DNAzyme Interactions: Design of A Nanoprobe for Fluorescent Detection Of Lead(II) Ions with High Sensitivity, Selectivity and Tunable Dynamic Range. *Chem. Commun.* **2011**, *47*, 6278−6280.
(19) Chang, H. X.; Tang, L. H.; Wang, Y.; Jiang, J. H.; Li, J. H. Graphene Fluorescence Resonance Energy Transfer Aptasensor for The Thrombin Detection. *Anal. Chem.* **2010**, *82*, 2341−2346.
(20) Chen, C. F.; Zhao, J. J.; Jiang, J. H.; Yu, R. Q. A Novel Exonuclease III-Aided Amplification Assay for Lysozyme Based on Graphene Oxide Platform. *Talanta* **2012**, *101*, 357−361.
(21) Hong, B. J.; An, Z.; Compton, O. C.; Nguyen, S. T. Tunable Biomolecular Interaction and Fluorescence Quenching Ability of Graphene Oxide: Application to "Turn-On" DNA Sensing in Biological Media. *Small* **2012**, *8*, 2469−2476.
(22) Treff, N. R.; Su, J.; Tao, X.; Levy, B.; Scott, R. T. Accurate Single Cell 24 Chromosome Aneuploidy Screening Using Whole Genome Amplification and Single Nucleotide Polymorphism Microarrays. *Fertil. Steril.* **2010**, *94*, 2017−2021.
(23) Garvin, M. R.; Saitoh, K.; Gharrett, A. J. Application of Single Nucleotide Polymorphisms to Non-Model Species: A Technical Review. *Mol. Ecol. Resour.* **2010**, *10*, 915−934.
(24) Zhao, X. J.; Li, C.; Paez, J. G.; Chin, K.; Janne, P. A.; Chen, T. H.; Girard, L.; Minna, J.; Christiani, D.; Leo, C.; Gray, J. W.; Sellers, W. R.; Meyerson, M. An Integrated View of Copy Number and Allelic Alterations in the Cancer Genome Using Single Nucleotide Polymorphism Arrays. *Cancer Res.* **2004**, *64*, 3060−3071.
(25) Seeb, J. E.; Carvalho, G.; Hauser, L.; Naish, K.; Roberts, S.; Seeb, L. W. Single-Nucleotide Polymorphism (SNP) Discovery and Applications of SNP Genotyping in Nonmodel Organisms. *Mol. Ecol. Resour.* **2011**, *11*, 1−8.
(26) Ku, C. S.; Loy, E. Y.; Salim, A.; Pawitan, Y.; Chia, K. S. The Discovery of Human Genetic Variations and Their Use as Disease Markers: Past, Present and Future. *J. Hum. Genet.* **2010**, *55*, 403−415.

(27) Chen, K.; Rajewsky, N. The Evolution of Gene Regulation by Transcription Factors and MicroRNAs. *Nat. Rev. Genet.* **2007**, *8*, 93−103.
(28) Shenouda, S. K.; Alahari, S. K. MicroRNA Function in Cancer: Oncogene or A Tumor Suppressor? *Cancer Metast. Rev.* **2009**, *28*, 369−378.
(29) Inui, M.; Martello, G.; Piccolo, S. MicroRNA Control of Signal Transduction. *Nat. Rev. Mol. Cell Biol.* **2010**, *11*, 252−263.
(30) Iorio, M. V.; Croce, C. M. MicroRNA Dysregulation in Cancer: Diagnostics, Monitoring and Therapeutics. A Comprehensive Review. *EMBO Mol. Med.* **2012**, *4*, 143−159.
(31) Lee, Y. S.; Dutta, A. MicroRNAs in Cancer. *Annu. Rev. Pathol.: Mech. Dis.* **2009**, *4*, 199−227.
(32) Krol, J.; Loedige, I. The Widespread Regulation of MicroRNA Biogenesis, Function and Decay. *Nat. Rev. Genet.* **2010**, *11*, 597−610.
(33) Liu, X. Q.; Aizen, R.; Freeman, R.; Yehezkeli, O.; Willner, I. Multiplexed Aptasensors and Amplified DNA Sensors Using Functionalized Graphene Oxide: Application for Logic Gate Operations. *ACS Nano* **2012**, *6*, 3553−3563.
(34) Zhou, G. H.; Zhang, X.; Ji, X. H.; He, Z. K. Ultrasensitive Detection of Small Molecule-Protein Interaction via Terminal Protection of Small Molecule Linked DNA and Exo III-Aided DNA Recycling Amplification. *Chem. Commun.* **2013**, *49*, 8854−8856.
(35) Liu, X. Q.; Freeman, R.; Willner, I. Amplified Fluorescence Aptamer-Based Sensors Using Exonuclease III for the Regeneration of the Analyte. *Chem.—Eur. J.* **2012**, *18*, 2207−2211.
(36) Marcano, D. C.; Kosynkin, D. V.; Berlin, J. M.; Sinitskii, A.; Sun, Z. Z.; Slesarev, A.; Alemany, L. B.; Lu, W.; Tour, J. M. Improved Synthesis of Graphene Oxide. *ACS Nano* **2010**, *4*, 4806−4814.
(37) Hummers, W. S.; Offeman, R. E. Preparation of Graphitic Oxide. *J. Am. Chem. Soc.* **1958**, *80*, 1339−1339.
(38) Waldman, T.; Kinzler, K. W.; Vogelstein, B. p21 is Necessary for the p53-Mediated G1 Arrest in Human Cancer Cells. *Cancer Res.* **1995**, *55*, 5187−5190.
(39) Simms, D.; Cizdziel, P.; Chomczynski, P. Trizol: A New Reagent for Optimal Single-Step Isolation of RNA. *Focus* **1993**, *15*, 99−102.
(40) Warner, J. H.; Rummeli, M. H.; Ge, L.; Gemming, T.; Montanari, B.; Harrison, N. M.; Buchner, B.; Briggs, G. A. D. Structural Transformations in Graphene Studied with High Spatial and Temporal Resolution. *Nat. Nanotechnol.* **2009**, *4*, 500−504.
(41) Kudin, K. N.; Ozbas, B.; Schniepp, H. C.; Prud'homme, R. K.; Aksay, I. A.; Car, R. Raman Spectra of Graphite Oxide and Functionalized Graphene Sheets. *Nano Lett.* **2008**, *8*, 36−41.
(42) Lu, C. H.; Li, J. A.; Lin, M. H.; Wang, Y. W.; Yang, H. H.; Chen, X.; Chen, G. N. Amplified Aptamer-Based Assay through Catalytic Recycling of the Analyte. *Angew. Chem., Int. Ed.* **2010**, *49*, 8454−8457.
(43) Zhang, X.-F.; Li, F. Interaction of Graphene with Excited and Ground State Rhodamine Revealed by Steady State and Time Resolved Fluorescence. *J. Photochem. Photobiol., A* **2012**, *246*, 8−15.
(44) Pang, Y.; Cui, Y.; Ma, Y.; Qian, H.; Shen, X. Fluorescence Quenching of Cationic Organic Dye by Graphene: Interaction and its Mechanism. *Micro Nano Lett.* **2012**, *7*, 608−612.
(45) Fan, Q.; Zhao, J.; Li, H.; Zhu, L.; Li, G. X. Exonuclease III-Based and Gold Nanoparticle-Assisted DNA Detection with Dual Signal Amplification. *Biosens. Bioelectron.* **2012**, *33*, 211−215.
(46) Jang, H.; Kim, Y. K.; Kwon, H. M.; Yeo, W. S.; Kim, D. E.; Min, D. H. A Graphene-Based Platform for the Assay of Duplex-DNA Unwinding by Helicase. *Angew. Chem., Int. Ed.* **2010**, *49*, 5703−5707.
(47) Bai, L. J.; Yuan, R.; Chai, Y. Q.; Zhuo, Y.; Yuan, Y. L.; Wang, Y. Simultaneous Electrochemical Detection of Multiple Analytes Based on Dual Signal Amplification of Single-Walled Carbon Nanotubes and Multi-Labeled Graphene Sheets Biomaterials. *Biomaterials* **2012**, *33*, 1090−1096.
(48) Chen, Y.; Jiang, B. Y.; Xiang, Y.; Chai, Y. Q.; Yuan, R. Target Recycling Amplification for Sensitive and Label-Free Impedimetric Genosensing Based on Hairpin DNA and Graphene/Au Nanocomposites. *Chem. Commun.* **2011**, *47*, 12798−12800.
(49) Saiki, R. K.; Scharf, S.; Faloona, F.; Mullis, K. B.; Horn, G. T. Enzymatic Amplification of Beta-Globin Genomic Sequences and Restriction Site Analysis for Diagnosis of Sickle Cell Anemia. *Science* **1985**, *230*, 1350−1354.
(50) Wu, D. Y.; Ugozzoli, L.; Pal, B. K.; Wallace, R. B. Allele-Specific Enzymatic Amplification of Beta-Globin Genomic DNA for Diagnosis of Sickle Cell Anemia. *Proc. Natl. Acad. Sci. U.S.A.* **1989**, *86*, 2757−2760.
(51) Guo, Y. J.; Deng, L.; Li, J.; Guo, S. J.; Wang, E. K.; Dong, S. J. Hemin−Graphene Hybrid Nanosheets with Intrinsic Peroxidase-like Activity for Label-free Colorimetric Detection of Single-Nucleotide Polymorphism. *ACS Nano* **2011**, *5*, 1282−1290.
(52) Lermo, A.; Campoy, S.; Barbe, J.; Hernandez, S.; Alegret, S.; Pividori, M. I. In situ DNA Amplification with Magnetic Primers for the Electrochemical Detection of Food Pathogens. *Biosens. Bioelectron.* **2007**, *22*, 2010−2017.
(53) Kato, D.; Sekioka, N.; Ueda, A.; Kurita, R.; Hirono, S.; Suzuki, K.; Niwa, O. Nanohybrid Carbon Film for Electrochemical Detection of SNPs Without Hybridization or Labeling. *Angew. Chem., Int. Ed.* **2008**, *47*, 6681−6684.
(54) Ermini, M. L.; Mariani, S.; Scarano, S.; Campa, D.; Barale, R.; Minunni, M. Single Nucleotide Polymorphism Detection by Optical DNA-Based Sensing Coupled with Whole Genomic Amplification. *Anal. Bioanal. Chem.* **2013**, *405*, 985−993.
(55) Hermeking, H. The miR-34 Family in Cancer and Apoptosis. *Cell Death Differ.* **2010**, *17*, 193−199.
(56) Dutta, K. K.; Zhong, Y.; Liu, Y. T.; Yamada, T.; Akatsuka, S.; Hu, Q.; Yoshihara, M.; Ohara, H.; Takehashi, M.; Shinohara, T.; Masutani, H.; Onuki, J.; Toyokuni, S. Association of microRNA-34a Overexpression with Proliferation is Cell Type-Dependent. *Cancer Sci.* **2007**, *98*, 1845−1852.
(57) Li, L. S.; Xie, X. H.; Luo, J. M.; Liu, M.; Xi, S. Y.; Guo, J. L.; Kong, Y. N.; Wu, M. Q.; Gao, J.; Xie, Z. M.; Tang, J.; Wang, X.; Wei, W. D.; Yang, M. T.; Hung, M. C.; Xie, X. M. Targeted Expression of miR-34a Using The T-VISA System Suppresses Breast Cancer Cell Growth and Invasion. *Mol. Ther.* **2012**, *20*, 2326−2334.
(58) Kato, M.; Paranjape, T.; Ullrich, R.; Nallur, S.; Gillespie, E.; Keane, K.; Esquela-Kerscher, A.; Weidhaas, J. B.; Slack, F. J. The mir-34 microRNA is Required for the DNA Damage Response in Vivo in C. Elegans and in Vitro in Human Breast Cancer Cells. *Oncogene* **2009**, *28*, 2419−2424.
(59) Yang, S.; Li, Y.; Gao, J.; Zhang, T.; Li, S.; Luo, A.; Chen, H.; Ding, F.; Wang, X.; Liu, Z. MicroRNA-34 Suppresses Breast Cancer Invasion and Metastasis by Directly Targeting Fra-1. *Oncogene* **2013**, *32*, 4294−4303.
(60) Chang, T.; Wentzel, E.; Kent, O.; Ramachandran, K.; Mullendore, M.; Lee, K.; Feldmann, G.; Yamakuchi, M.; Ferlito, M.; Lowenstein, C.; Arking, D.; Beer, M.; Maitra, A.; Mendell, J. Transactivation of miR-34a by p53 Broadly Influences Gene Expression and Promotes Apoptosis. *Mol. Cell* **2007**, *26*, 745−752.
(61) Yamakuchi, M.; Ferlito, M.; Lowenstein, C. J. miR-34a Repression of SIRT1 Regulates Apoptosis. *Proc. Natl. Acad. Sci. U.S.A.* **2008**, *105*, 13421−13426.
(62) Lu, Z. X.; Zhang, L. M.; Deng, Y.; Li, S.; He, N. Y. Graphene Oxide for Rapid microRNA Detection. *Nanoscale* **2012**, *4*, 5840−5842.
(63) Dong, H. F.; Zhang, J.; Ju, H. G.; Lu, H. T.; Wang, S.; Jin, S.; Hao, K. H.; Du, H. W.; Zhang, X. J. Highly Sensitive Multiple microRNA Detection Based on Fluorescence Quenching of Graphene Oxide and Isothermal Strand-Displacement Polymerase Reaction. *Anal. Chem.* **2012**, *84*, 4587−4593.
(64) Yang, L.; Liu, C. G.; Ren, W.; Li, Z. P. Graphene Surface-Anchored Fluorescence Sensor for Sensitive Detection of MicroRNA Coupled with Enzyme-Free Signal Amplification of Hybridization Chain Reaction. *ACS Appl. Mater. Interfaces* **2012**, *4*, 6450−6453.
(65) Cui, L.; Lin, X. Y.; Lin, N. H.; Song, Y. L.; Zhu, Z.; Chen, X.; Yang, C. J. Graphene Oxide-Protected DNA Probes for Multiplex microRNA Analysis in Complex Biological Samples based on A Cyclic Enzymatic Amplification Method. *Chem. Commun.* **2012**, *48*, 194−196.

(66) Ryoo, S.-R.; Lee, J.; Yeo, J.; Na, H.-K.; Kim, Y.-K.; Jang, H. J.; Lee, J. H.; Han, S. W.; Lee, Y.-H.; Kim, V. N.; Min, D.-H. Quantitative and Multiplexed MicroRNA Sensing in Living Cells Based on Peptide Nucleic Acid and Nano Graphene Oxide (PANGO). *ACS Nano* **2013**, *7*, 5882−5891.
(67) Zhu, X.; Zhou, X. M.; Xing, D. Label-Free Detection of MicroRNA: Two-Step Signal Enhancement with a Hairpin-Probe-Based Graphene Fluorescence Switch and Isothermal Amplification. *Chem.—Eur. J.* **2013**, *19*, 5487−5494.
(68) Tu, Y. Q.; Li, W.; Wu, P.; Zhang, H.; Cai, C. X. Fluorescence Quenching of Graphene Oxide Integrating with the Site-Specific Cleavage of the Endonuclease for Sensitive and Selective MicroRNA Detection. *Anal. Chem.* **2013**, *85*, 2536−2542.